Contents lists available at ScienceDirect

# Vibrational Spectroscopy

# Characterization of dental fragments of *Toxodon* sp. (Mammalia, Notoungulata) by multiple physical and chemical techniques

Edher Zacarias Herrera [a,b,]*, Sergio D. Rios [c], Celeste Aquino Ayala [a], Christian Colman [d], Ricardo Souberlich [e], María Luisa Idoyaga [f], Christian J. Sánchez [a,f], Avacir Casanova Andrello [g], Alexandre Mello [b]

[a] *Laboratorio de Análisis Molecular y Elemental, Facultad de Ciencias Exactas y Naturales, Universidad Nacional de Asunción, Paraguay*
[b] *Department of Condensed Matter, Applied Physics and Nanoscience, Brazilian Center for Research in Physics (CBPF), Brazil*
[c] *Departamento de Arqueología y Paleontología, Secretaría Nacional de Cultura, Asunción, Paraguay*
[d] *Centro de Investigación Esquel de Montaña y Estepa Patagónica (CONICET-UNPSJB), Esquel, Chubut, Argentina*
[e] *Laboratorio de Paleontología, Facultad de Ciencias Exactas y Naturales, Universidad Nacional de Asunción, Paraguay*
[f] *Comisión Nacional de Energía Atómica, Paraguay*
[g] *State University of Londrina, Department of Physics, Londrina, Paraná, Brazil*

## ARTICLE INFO

## ABSTRACT

In this work, there were analyzed dental remains of a *Toxodon* sp. (Mammalia, Notoungulata) specimen rescued from the riverbank of the Ypané River in Paraguay. Several techniques were used to analyze the different geological aspects of the samples, thus providing keys to the understanding of fossilization processes and the implications of paleoenvironmental conditions in the apatites present in the dental remains. The identification of the chemical substances present in the sample was made by Raman and Fourier Transform Infrared (FTIR) spectroscopy, the chemical composition of the samples was determined using energy dispersive X-ray fluorescence (EDXRF) and X-ray photoelectron spectroscopy (XPS), and the mineralogy by X-ray Diffraction (XRD). It is worth mentioning that this work is the first in the area of Paleometry carried out in Paraguay.

## 1. Introduction

Bones and teeth have organic and mineral compounds consisting mainly of calcium phosphates (CaP). The chemical structure of these materials varies according to factors such as species type, density, and composition [1–4].

Hydroxyapatite (HA) is the main mineral existing in bones and teeth. Its chemical formula is $Ca_{10}(PO_4)_6(OH)_2$ [5,6]. This mineral absorbs easily different types of metallic and non-metallic elements from the environment, which are incorporated within its structure [7–12].

The processes of diagenesis by which the fossil remains can be exposed are numerous and vary according to the environmental factors existing at the time of burial in addition to other intrinsic structural characteristics of the original material. In recent years, numerous works have analyzed the chemical, the elemental, and structural composition of fossil remains to understand and get to know better the bone structures of extinct animals and organics compounds [13–16].

Physical and chemical characterization of bones allows us to understand and explain the diagenetic process during their transformation to fossils and their interaction with the environment [13,17,18], and it also allows us to compare between extinct and modern specimens [19, 20].

In this work the dental remains of a *Toxodon* sp. (Mammalia, Notoungulata) from Quaternary sedimentary levels of Paraguay [21] were thoroughly characterized by multiple physical and chemical characterization techniques.

## 2. Methodology

### 2.1. Samples

For the analysis, were selected two fragments of dental remains

---

* Corresponding author at: Facultad de Ciencias Exactas y Naturales, San Lorenzo, Paraguay.
*E-mail addresses:* edher712@gmail.com (E.Z. Herrera), sergiord40@gmail.com (S.D. Rios), celes.aquino@gmail.com (C. Aquino Ayala), ccolmanpatino@comahue-conicet.gob.ar (C. Colman), rsouberlich@gmail.com (R. Souberlich), mlidoyaga@gmail.com (M.L. Idoyaga), cjsanchez@rec.una.py (C.J. Sánchez), acandrello@uel.br (A. Casanova Andrello), mello@cbpf.br (A. Mello).

belonging to *Toxodon* sp [22], which are deposited in the collections of the Paleontology Laboratory of the Facultad de Ciencias Exactas y Naturales (FACEN UNA) of Paraguay with codes Facen-vert-0113-A and Facen-vert-0113-B (Fig. 1.b).

The fragments correspond to sections of an upper left incisive and a molar that were collected on the right bank of the Paraguay River (23°35′S; 57°27′W) from a Quaternary sedimentary level, near Puerto Santa Rosa, department of San Pedro, very close to its border with the department of Concepción of Paraguay [21].

These remains were considered viable for analysis since they were not contaminated with chemicals generally used for conservation (consolidators, glues, etc.). Also, due to their lack of preparation, it was possible to extract small fragments that would then be pulverized for their corresponding characterization.

## 2.2. Characterization studies

The powder surface characterization was determined by X-Ray photoelectron Spectroscopy (XPS) with PHOIBOS 100/150 analyzer manufactured by SPECS co. With aluminum X-Ray tube (Kα Al 1486 eV). Data processing was performed using the Casa-XPS software.

Energy Dispersive X-Ray Fluorescence (EDXRF) system model EDX-7000 with Rh target manufactured by Shimadzu was used for the semi-qualitative analysis of the elements that make up the entire parts analyzed. There were chosen 5 random points from the samples and then was calculated the average.

The Raman and Infrared Absorption characterization of the vibrational properties of samples by Fourier transform Infrared Spectroscopy (FTIR) was made using a spectrometer model Nicolet™ iS5. The samples, that were pelletized under a 2 ton. pressure, with KBr, were FTIR analyzed under absorbance mode within the 400 to 4000 $cm^{-1}$ range, with a resolution of 4 $cm^{-1}$.

The Raman spectra were recorded using a Raman BWS415−785S system (B&WTek), with a 785 nm, 300 mW laser that was directly shone on the flat surfaces of the fossil remains by contact of the acquisition probe with a measurement range from 250 to 3000$cm^{-1}$ and a resolution of 4 $cm^{-1}$. The acquisitions time was adjusted for spectrum optimization.

X-ray diffraction patterns were collected with a Panalytical XPert PRO system with Cu Kα-radiation (λ =1.5418 Å). The measurements were done with powder material and the crystalline phases identified by comparison of the calculated reflections with the ICSD (Inorganic Crystal Structures Database), with code 26204 that indicates the theoretical position of the crystalline phases of the structural model.

## 3. Results

The Apatitic nature of the samples were demonstrated by X-ray diffraction, the typical patterns of the samples Facen-vert-0113-A and Facen-vert-0113-B are shown in Fig. 2, the patterns are indexed with the main lines of reflections.

The presence of $(PO_4)^{3-}$ the functional groups were detected by FTIR and Raman spectroscopy in addition to the presence of organic groups and carbonates, as seen in Figs. 3 and 4.
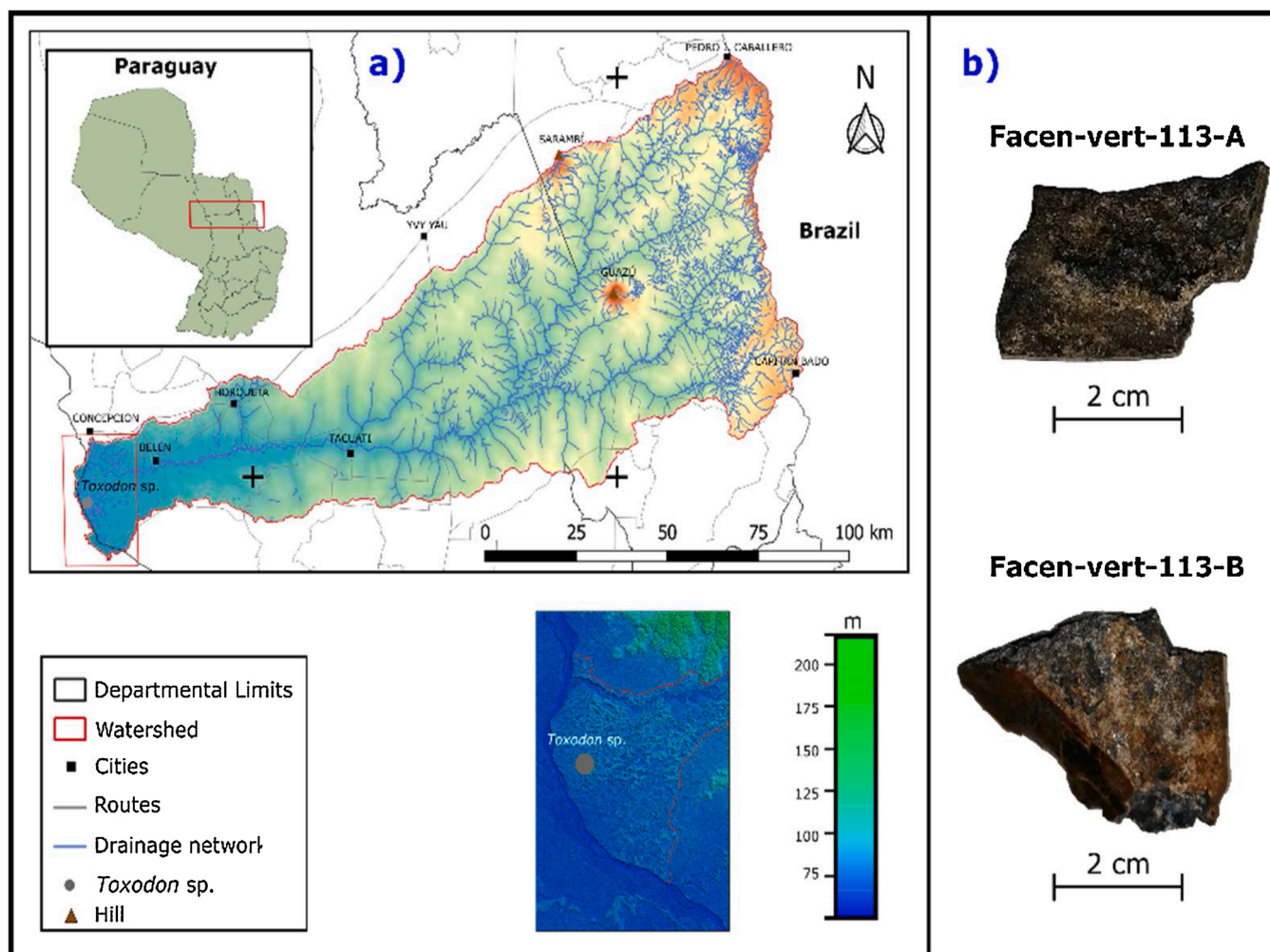


**Fig. 1. a)** The location of the fossil site in Puerto Santa Rosa and the Ypané river basin b) Dental fragments belonging of *Toxodon* sp.
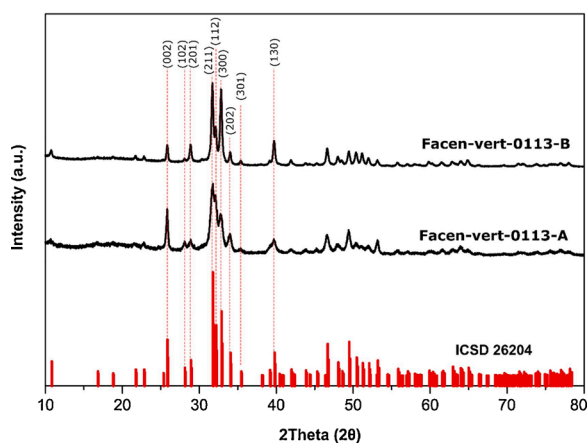
**Fig. 2.** XRD patterns of the Facen-vert-0113-A and Facen-vert-0113-B samples compared with the calculated reflections of ICSD 26,204 for ($\lambda$ =1.5418 Å, corresponding to Cu-K$\alpha$).
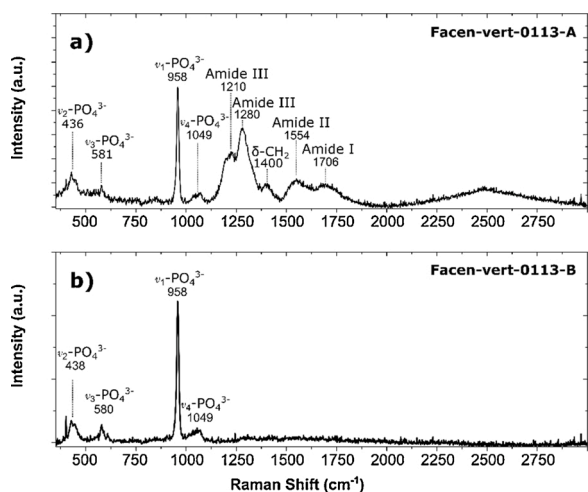


**Fig. 3.** Raman spectra of a) Facen-vert-0113-A and b) Facen-vert-0113-B indicating the active bands.
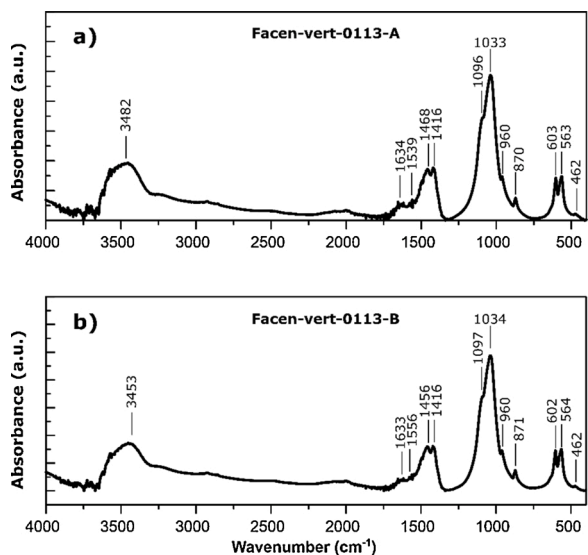


**Fig. 4.** FTIR spectra of a) Facen-vert-0113–A and b) Facen-vert-0113-B samples.

Raman spectra of the Facen-vert-0113-A samples showed the presence of organic components (Amide I, Amide II and Amide III) and carbonates while the Facen-vert-0113-B sample lacks (Table 1).

FTIR spectra also indicate the presence of $(PO_4)^{3-}$ phosphate groups, $(CO_3)^{2-}$ carbonates, in addition to the presence of Organic groups such as Amide I and Amide II (Table 2).

FTIR characterization, which spectra and band assignment are displayed in Fig. 4 and Table 2, respectively. FTIR spectra of the samples further indicates the presence of phosphate and carbonate groups in the samples.

The surface analysis of the powder samples was done by XPS, the Ca, P, O, Zn and C elements characteristic peaks of interest were distinguished as commonly found in bio-apatite [43,44]. The survey spectra and the acquired spectra of high resolution of elements of interest are presented in Figs. 5 and 6.

The O 1s, Ca 2p and P 2p high resolution spectra, recorded from the Facen-vert-0113-A samples and displayed in Fig. 5, allowed the identification, of the probable surface chemical composition present in the fossilized samples. The O 1s region was found to be deconvoluted into two peaks which centroids are at 530.9 eV and 528.6 eV. The former deconvoluted peak may be correlated with oxygen in $(PO_4)^{3-}$, OH- and $(CO_3)^{2-}$ groups. The latter peak is associated with the contributions of other elements with chemical bonds with O [45–48]. This can cause a dislocation in the spectra, which interferes with the identification of the tested compounds.

In the case of P 2p$_{3/2}$, the center of the adjustment peak is 132.9 eV, which is associated with the group $(PO_4)^{3-}$ usually encountered in the apatite structures [46–48].

The center of the adjustment peak of Ca 2p$_{3/2}$ in 347.1 eV may be attributed to Ca-O, Ca—OH bonds and to Ca-Ca structures [46–48].

The Facen-vert-0113-B high resolution spectra of O 1s, have two peaks of adjustments that were necessary for the deconvolution, the first with center at 330.8 eV associated to $(PO_4)^{3-}$, OH- groups and $(CO_3)^{2-}$ [45–47], and the second with center at 528.7 eV are due to the contribution of the other elements present in the sample. In the P 2p$_{3/2}$ high resolution spectrum the center of the adjustment peak is 132.8 eV, which is associated with the $(PO_4)^{3-}$ group, usually encountered in apatite structures [46–48]. The center of the adjustment peak of Ca 2p$_{3/2}$ in 346.1 eV can be attributed to Ca-O, Ca-OH bonds and to Ca-Ca structures [46–48].

The elements Zn, O, Ca, C and P were identified in the analyzed samples as indicated in Figs. 4 and 5. A belonging to Survey, the utilized

**Table 1**
Raman-active bands found in Facen-vert-0113-A and Facen-vert-0113-B samples.

| Samples | Assignment | Reference |
|---|---|---|
| Facen-vert-0113 –A | | |
| ne | Flexion mode ($\nu_2$) of the (PO₄) group | [23–26] |
| 581 | Triple degenerate folding mode ($\nu_4$) of group (PO₄) (bond O—P–O) | [24,27,28] |
| 958 | P-O stretch mode ($\nu_1$) of the (PO₄) group | [23,24,29] |
| 1049 | Stretch mode P-O ($\nu_3$) of the (PO₄) group | [23,24] |
| 1210 | Amide III | [30,31,32, 33] |
| 1280 | Amide III | [30,31,32, 33] |
| 1400 | $(CO_3)^{2-}$ | [30,34,35] |
| 1554 | Amide II | [36,37] |
| 1706 | Amide I | [30,31] |
| | | |
| Facen-vert-0113-B | | |
| 438 | P-O stretch mode ($\nu_2$) of the (PO₄) group | [23–26] |
| 580 | Triple degenerate folding mode ($\nu_4$) of group (PO₄) (bond O—P–O) | [24,27,28] |
| 958 | P-O stretch mode ($\nu_1$) of the (PO₄) group | [23,24,29] |
| 1049 | Stretch mode P-O ($\nu_3$) of the (PO₄) group | [23,24] |

**Table 2**

Assignation in the FTIR bands of the Facen-vert-0113-A and Facen-vert-0113-B.

| Samples | Assignment | Reference |
|---|---|---|
| Facen-vert-0113-A | | |
| 462 | Double degenerated bending mode ($\nu_2$) of the O-P-O O-P-Obonds of the ($PO_4$) | [29,38,39] |
| 563 | Triply degenerated bending mode, ($\nu_4$), of the O-P-O bonds of the ($PO_4$) group | [29,38] |
| 603 | Triply degenerated bending mode, ($\nu_4$), of the O-P-O bonds of the ($PO_4$) group | [29,38] |
| 870 | Characteristic peak of hydrogen phosphate group (nondistinguishable peak) | [6,40] |
| 960 | Non degenerated symmetric stretching mode, ($\nu_1$), of the P-O bonds of the ($PO_4$) | [40,41] |
| 1033 | Triply degenerated asymmetric stretching mode, ($\nu_3$), of the P-O bond of the ($PO_4$) | [29,38] |
| 1096 | Occur in non-stoichiometric apatites containing $(HPO_4)^{2-}$ ions or $(CO_3)^{2-}$ | [29,39] |
| 1416 | Stretching mode ($\nu_1$) of the group $(CO_3)^{2-}$ and $CH_2$ wag (Organic) | [42] |
| 1468 | Amide II (Organic) | [29,39] |
| 1634 | Amide I (Organic) | [29,39] |
| 3482 | $\nu$ OH$^-$ | [29,39] |
| Facen-vert-0113 -B | | |
| 462 | Double degenerated bending mode ($\nu_2$) of the O-P-O bonds of the ($PO_4$) | [29,38,39] |
| 564 | Triply degenerated bending mode, ($\nu_4$), of the O-P-O bonds of the ($PO_4$) group | [29,38,39] |
| 602 | Triply degenerated bending mode, ($\nu_4$), of the O-P-O bonds of the ($PO_4$) group | [29,38] |
| 871 | Characteristic peak of hydrogen phosphate group (nondistinguishable peak) | [40,41] |
| 960 | Non degenerated symmetric stretching mode, ($\nu_1$), of the P-O bonds of the ($PO_4$) | [40,41] |
| 1034 | Triply degenerated asymmetric stretching mode, ($\nu_3$), of the P-O bond of the ($PO_4$) | [29,38] |
| 1097 | Triply degenerated asymmetric stretching mode, ($\nu_3$), of the P-O bond of the ($PO_4$) | [29,39] |
| 1416 | Stretching mode ($\nu_1$) of the group $(1d436;1d442;_3)^{2-}$ and $CH_2$ wag (Organic) | [42] |
| 1456 | Amide II (Organic) | [29,39] |
| 1633 | Amide I (Organic) | [29,39] |
| 3456 | $\nu$ OH$^-$ | [29,39] |

regions are indicated to the quantification of the mentioned elements and presented with their respective deviations in the Table 3 in (At%).

Through the obtained values in Table 3, proportions of Ca and P were calculated for the Facen-vert-0113-A and Facen-vert-0113-B samples resulting in 1.59 and 1.58.

Semi-quantitative analysis by EDXRF of the elements in the samples was performed. The characteristic (Fig. 7), and the major element intensity calculated are shown in Table 4.

## 4. Discussion

The XRD allows us to identify the crystalline shape structure of the analyzed samples, on which both HA were identified. A more detailed analysis with this technique using a Rietveld refinement can calculate the unitary cell parameters of the analyzed material and provide information of substitutions and/or defects of the crystalline analyzed material. This analytical process escapes the limitations of the authors.

The probable presence of calcite may correspond to the events of material deposition through external environmental factors and may not have its origin in the fossil. The material analyzed was obtained in a flood zone near the Paraguay River, which is subject to periodic rises and falls in water levels. These factors favored the precipitation of calcite that could penetrate the pores of the analyzed material and its surface since in periods of low water level it would remain stagnant with the carbonate concentrations [49–51].

The relations of Ca/P in both samples indicate that they are apatite's due to the proportion of Ca/P they possess [52]. The presence of Zn can

also be due to the inclusion of this abundant element in the environment during the processes that the dents were subdued during the diagenesis and/or the presence of this element in the original structure of the analyzed samples [5,53–55].

The XPS and XRF techniques provide information about the elemental and the binding energies of elements in the analyzed material in the case of XPS. The results exposed in Tables 3 and 4 show that the amount of detected and quantified elements is reduced in the XPS compared to the EDXRF. This is because XPS is a surface technique. Besides having lower sensitivity to heavy elements and higher to light elements, the EDXRF technique allows us to measure the sample at bulk, and it possesses high sensitivity to heavy elements but not to the light elements.

As dental material, the detection of F was a possibility, but it was not detected in the XPS and the EDXRF does not have the sensitivity to detect it.

The presence of elements such as U, Ba, Y and Sr in the EDXRF may be correlated to the fossil outcrop, which in turn is limited by the morphogenetic conditions of the area. To explain the presence of these elements attached to the remains, it must be considered a much broader geographic context than the fossil lying area (Fig. 1. Map of the basin). We considered two fundamental factors; first, the morphological expression of the remains, which suffered a low or medium intensity water transport. Second, the presence of the Ypané river basin, which empties into the Paraguay river in the form of a currently stabilized river fan and considerable dimensions in the vicinity of the fossil site.

Considering the good state of conservation of the fossil dental remains, they were found probably not very far from the primary depositional site. It cannot be elucidated whether the deposit is genetically related to the Paraguay river or the Ypané river delta since they are both connected in certain seasonal events. The Ypané river basin has a linear extension of more than 180 km, beginning in the limits with Brazil, in the eastern sector of the northeast of Eastern Paraguay and drains in the W direction until ending in the Paraguay river in the form of a fluvial fan. The head of the basin is located to the east of the Alkaline Province of Amambay where the previously mentioned elements are much more common [56–62].

Physical-chemical analyzes mentioned that the mineralogy of the fossils is totally modified by the diagenetic process, but that the results also reveal that the composition of the bones is similar to the deposits from which they were extracted. Therefore, it is not strange that the deposit, being within the Ypané River Basin, reflects the presence of elements outside the final deposition site, since these could come from the contribution areas of the large hydrographic basin, where they are located. They are 1 st, 2nd and 3rd order tributaries that practically cross the alkaline subcircular intrusive bodies "Cerro Sarambí and Cerro Guazú" in the northeast of the Eastern Region (Fig. 1, map of the basin).

## 5. Conclusion

The characterizations performed by XRD, XRF, Raman, FTIR and XPS spectroscopies on dental fragments of *Toxodon* sp. indicate that material is made up of apatite of similar chemical and mineral composition. The FTIR bands of the analyzed materials and the presence of other elements detected in the XPS and XRF measurements suggest that there is a probability of partial substitutions in the original bio-apatite. With FTIR and Raman spectroscopies, it is possible to rapidly and reliably identify the presence of the group $(PO_4)^{3-}$ and organics compounds that are common in bones and fossils. For the identification of substitutions and/or presence of other crystalline calcium phosphates, other analyzes are necessary.

We propose that the uncommon elements in the bio-apatite of the analyzed fossils could come from alkaline subcircular intrusive bodies and that, after being transported for more than 180 km in a SW direction they reached the Paraguay river, were incorporated into the bed of the Ypané river basin, near the site from which the fossils were extracted.
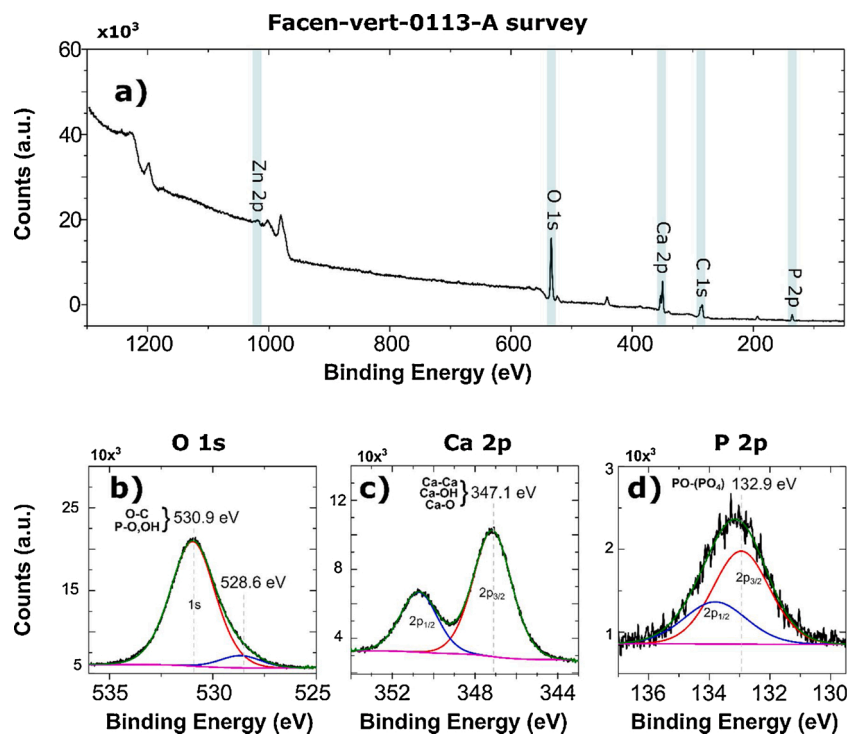
**Fig. 5.** XPS spectra of Facen-vert-0113-A samples a) survey spectra, high resolution spectra with their respective deconvolutions of b) O 1s, c) Ca 2p and d) P 2p.
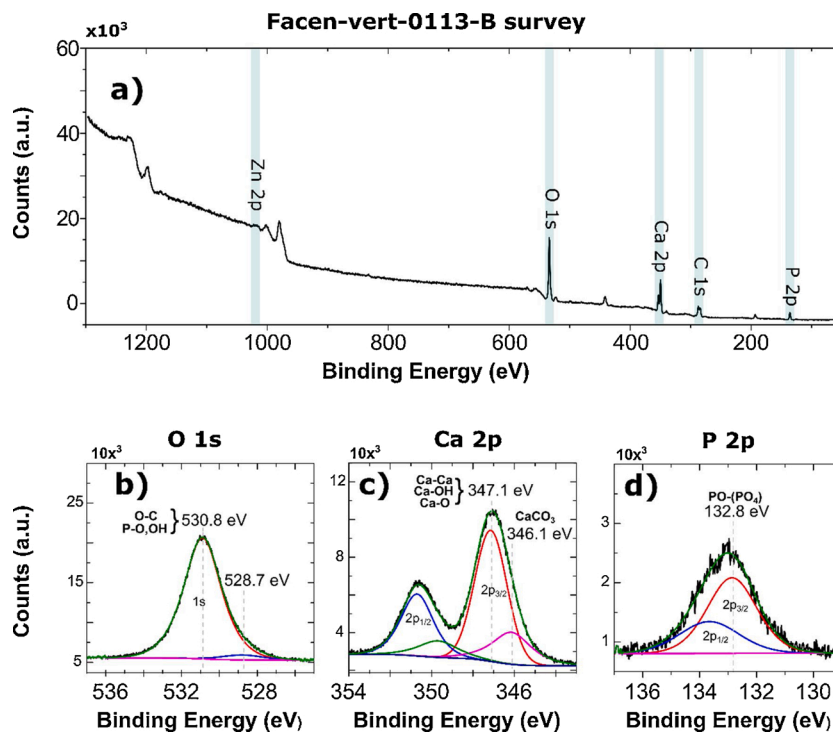


**Fig. 6.** XPS spectra of Facen-vert-0113-B samples a) survey spectra, high resolution spectra with their respective deconvolutions of b) O 1s, c) Ca 2p and d) P 2p.

**Table 3**

XPS survey quantifications of Facen-vert-0113-A and Facen-vert-0113-B samples.

| Sample | Elements (At%) | | | | |
|---|---|---|---|---|---|
| | O 1s | C 1s | Ca 2p | P 2p | Zn 2p |
| **Facen-vert-0113-A** | 41.75 ± 0.73 | 37.42 ± 0.91 | 12.61 ± 0.33 | 7.9 ± 0.43 | 0.29 ± 0.13 |
| **Facen-vert-0113-B** | 41.75 ± 0.79 | 34.74 ± 0.98 | 14.08 ± 0.38 | 8.88 ± 0.46 | 0.52 ± 0.28 |
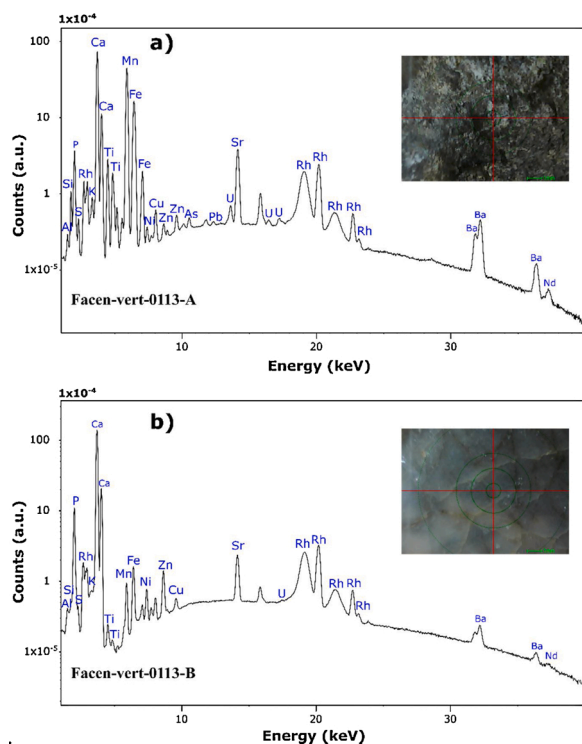


**Fig. 7.** XRF spectra of Facen-vert-0113–A and Facen-vert-0113-B samples.

**Table 4**

EDXRF elements intensities (cps/μA) of the Facen-vert-0113-A and Facen-vert-0113-B samples.

| Element | Facen-vert-0113 (cps/μA) | Facen-vert-0113 –B (cps/μA) |
|---|---|---|
| Al | 0.89 ± 0.33 | 1.28 ± 0.35 |
| Si | 3.47 ± 1.90 | 4.87 ± 3.08 |
| P | 33.70 ± 13.26 | 41.31 ± 16.08 |
| S | 0.61 ± 0.26 | — |
| K | 3.47 ± 0.95 | 4.24 ± 0.74 |
| Ca | 656.32 ± 158.55 | 766.58 ± 165.29 |
| Ti | — | 1.44 ± 1.80 |
| Mn | 192.57 ± 133.40 | 126.17 ± 244.09 |
| Fe | 116.22 ± 127.72 | 104.31 ± 135.58 |
| Cu | 2.65 ± 0.33 | 2.93 ± 0.78 |
| Zn | 4.65 ± 3.37 | 5.21 ± 2.91 |
| Sr | 26.41 ± 7.05 | 35.29 ± 18.71 |
| Y | 1.26 ± 0.44 | ND |
| Ba | 10.15 ± 8.81 | 3.35 ± 6.61 |
| U | 2.05 ± 1.32 | 3.98 ± 0.24 |

The obtained results allow us to establish a precedent regarding the physicochemical characterization studies on fossil remains of the South American quaternary and provide clues about the development of diagenesis processes and their composition.

## Statement of contributions

## Declaration of Competing Interest

The authors declare that they have no known competing financial interests or personal relationships that could have appeared to influence the work reported in this paper.

## Acknowledgments

## References

[1] J. Aerssens, S. Boonen, G. Lowet, J. Dequeker, Interspecies differences in bone composition, density, and quality: potential implications for in vivo bone research, Endocrinology 139 (1998) 663–670.

[2] I. Amenabar, S. Poly, W. Nuansing, E.H. Hubrich, A.A. Govyadinov, F. Huth, R. Krutokhvostov, L. Zhang, M. Knez, J. Heberle, A.M. Bittner, R. Hillenbrand, Structural analysis and mapping of individual protein complexes by infrared nanospectroscopy, Nat. Commun. 4 (2013) 2890, https://doi.org/10.1038/ncomms3890.

[3] K.A. Athanasiou, M.P. Rosenwasser, J.A. Buckwalter, T.I. Malinin, V.C. Mow, Interspecies comparisons of in situ intrinsic mechanical properties of distal femoral cartilage, J. Orthop. Res. 9 (1991) 330–340.

[4] F.C.M. Driessens, J.W.E. Van Dijk, J. Borggreven, Biological calcium phosphates and their role in the physiology of bone and dental tissues I. Composition and solubility of calcium phosphates, Calcif. Tissue Res. 26 (1978) 127–137.

[5] V.R. Martinez-Zelaya, L. Zarranz, E.Z. Herrera, A.T. Alves, M.J. Uzeda, E. Mavropoulos, A.L. Rossi, A. Mello, J.M. Granjeiro, M.D. Calasans-Maia, In vitro and in vivo evaluations of nanocrystalline Zn-doped carbonated hydroxyapatite/alginate microspheres: zinc and calcium bioavailability and bone regeneration, Int. J. Nanomedicine 14 (2019) 3471..

[6] S.J. Joris, C.H. Amberg, Nature of deficiency in nonstoichiometric hydroxyapatites. II. Spectroscopic studies of calcium and strontium hydroxyapatites, J. Phys. Chem. 75 (1971) 3172–3178.

[7] J.P. Lafon, E. Champion, D. Bernache-Assollant, Processing of AB-type carbonated hydroxyapatite Ca 10-x (PO 4) 6-x (CO 3) x (OH) 2-x-2y (CO 3) y ceramics with controlled composition, J. Eur. Ceram. Soc. 28 (2008) 139–147, https://doi.org/10.1016/j.jeurceramsoc.2007.06.009.

[8] S. Rengaraj, K.H. Yeon, S.H. Moon, Removal of chromium from water and wastewater by ion exchange resins, J. Hazard. Mater. 87 (2001) 273–287, https://doi.org/10.1016/S0304-3894(01)00291-6.

[9] Y. Takeuchi, H. Arai, Removal of coexisting Pb2+, Cu2+and Cd2+Ions from water by addition of hydroxyapatite powder, J. Chem. Eng. JAPAN. 23 (1990) 75–80, https://doi.org/10.1252/jcej.23.75.

[10] Q.Y. Ma, S.J. Tralna, T.J. Logan, J.A. Ryan, Effects of aqueous Al, Cd, Cu, Fe(II), Ni, and Zn on Pb immobilization by hydroxyapatite, Environ. Sci. Technol. 28 (1994) 1219–1228, https://doi.org/10.1021/es00056a007.

[11] T.-M.G. Chu, D.G. Orton, S.J. Hollister, S.E. Feinberg, J.W. Halloran, Mechanical and in Vivo Performance of Hydroxyapatite Implants with Controlled Architectures, 2002.

[12] H. Buettner, G.B. Bartley, Tissue breakdown and exposure associated with orbital hydroxyapatite implants, Am. J. Ophthalmol. 113 (1992) 669–673, https://doi.org/10.1016/S0002-9394(14)74792-0.

[13] G. Piga, A. Santos-Cubedo, A. Brunetti, M. Piccinini, A. Malgosa, E. Napolitano, S. Enzo, A multi-technique approach by XRD, XRF, FT-IR to characterize the diagenesis of dinosaur bones from Spain, Palaeogeogr. Palaeoclimatol. Palaeoecol. 310 (2011) 92–107.

[14] L. Merino, A.D. Buscalioni, Mineralogía y cambios composicionales en fragmentos óseos atribuidos a un dinosaurio ornitópodo del yacimiento barremiense de

Buenache de la Sierra (Formación Calizas de La Huérguina, Cuenca, España), Estud. Geológicos. (2013), https://doi.org/10.3989/egeol.41200.253.

[15] D.B. Thomas, R.E. Fordyce, R.D. Frew, K.C. Gordon, A rapid, non-destructive method of detecting diagenetic alteration in fossil bone using Raman spectroscopy, J. Raman Spectrosc. An Int. J. Orig. Work All Asp. Raman Spectrosc. Incl. High. Order Process. Also Brillouin Rayleigh Scatt. 38 (2007) 1533–1537.

[16] C.A.M. France, D.B. Thomas, C.R. Doney, O. Madden, FT-Raman spectroscopy as a method for screening collagen diagenesis in bone, J. Archaeol. Sci. 42 (2014) 346–355.

[17] P. Arkai, R.J. Merriman, B. Roberts, D.R. Peacor, M. Toth, Crystallinity, crystallite size and lattice strain of illite-muscovite and chlorite: comparison of XRD and TEM data for diagenetic to epizonal pelites, Eur. J. Mineral. 8 (1996) 1119–1137.

[18] D.K. McCarty, B.A. Sakharov, V.A. Drits, Early clay diagenesis in Gulf Coast sediments: new insights from XRD profile modeling, Clays Clay Miner. 56 (2008) 359–379.

[19] A. Bartsiokas, A.P. Middleton, Characterization and dating of recent and fossil bone by X-ray diffraction, J. Archaeol. Sci. 19 (1992) 63–72, https://doi.org/10.1016/0305-4403(92)90007-P.

[20] J.A. Lee-Thorp, N.J. van der Merwe, Aspects of the chemistry of modern and fossil biological apatites, J. Archaeol. Sci. 18 (1991) 343–354.

[21] S.D. Rios, MamÍFeros del cuaternario de puerto santa Rosa, departamento De San Pedro, Paraguay, Boletín Del Mus. Nac. Hist. Nat. Del Paraguay. 18 (1) (2014) 100–110.

[22] R. Owen, A description of the cranium of the toxodon platensis, a gigantic extinct mammiferous species, referable by its dentition to the rodentia, but with affinities to the pachydermata and the herbivorous cetacea, Proc. Geol. Soc. London (1837) 541–542.

[23] G.R. Sauer, W.B. Zunic, J.R. Durig, R.E. Wuthier, Fourier transform Raman spectroscopy of synthetic and biological calcium phosphates, Calcif. Tissue Int. 54 (1994) 414–420.

[24] H. Tsuda, J. Arends, Raman spectra of human dental calculus, J. Dent. Res. 72 (1993) 1609–1613.

[25] B.O. Fowler, M. Markovic, W.E. Brown, Octacalcium phosphate. 3. Infrared and Raman vibrational spectra, Chem. Mater. 5 (1993) 1417–1423.

[26] B. Mihailova, B. Kolev, C. Balarew, E. Dyulgerova, L. Konstantinov, Vibration spectroscopy study of hydrolyzed precursors for sintering calcium phosphate bio-ceramics, J. Mater. Sci. 36 (2001) 4291–4297.

[27] W.P. Griffith, Raman studies on rock-forming minerals. Part II. Minerals containing MO 3, MO 4, and MO 6 groups, J. Chem. Soc. A Inorganic, Phys. Theor. (1970) 286–291.

[28] P.N. De Aza, F. Guitian, C. Santos, S. De Aza, R. Cusco, L. Artus, Vibrational properties of calcium phosphate compounds. 2. Comparison between hydroxyapatite and β-tricalcium phosphate, Chem. Mater. 9 (1997) 916–922.

[29] B.O. Fowler, Infrared studies of apatites. I. Vibrational assignments for calcium, strontium, and barium hydroxyapatites utilizing isotopic substitution, Inorg. Chem. 13 (1974) 194–207.

[30] G. Penel, C. Delfosse, M. Descamps, G. Leroy, Composition of bone and apatitic biomaterials as revealed by intravital Raman microspectroscopy, Bone. 36 (2005) 893–901.

[31] M. Kazanci, P. Fratzl, K. Klaushofer, E.P. Paschalis, Complementary Information on In Vitro Conversion of Amorphous (Precursor) Calcium Phosphate to Hydroxyapatite from Raman Microspectroscopy and Wide-Angle X-Ray Scattering, (n.d.). https://doi.org/10.1007/s00223-006-0011-9.

[32] M. Tsuboi, Y. Kubo, K. Akahane, J.M. Benevides, G.J. Thomas, Determination of the amide I raman tensor for the antiparallel β-sheet: application to silkworm and spider silks, J. Raman Spectrosc. 37 (2006) 240–247, https://doi.org/10.1002/jrs.1452.

[33] D. Kurouski, T. Postiglione, T. Deckert-Gaudig, V. Deckert, I.K. Lednev, Amide i vibrational mode suppression in surface (SERS) and tip (TERS) enhanced Raman spectra of protein specimens, Analyst 138 (2013) 1665–1673, https://doi.org/10.1039/c2an36478f.

[34] E.A. Schauble, P. Ghosh, J.M. Eiler, Preferential formation of 13C–18O bonds in carbonate minerals, estimated using first-principles lattice dynamics, Geochim. Cosmochim. Acta 70 (2006) 2510–2529.

[35] A. Antonakos, E. Liarokapis, T. Leventouri, Micro-Raman and FTIR studies of synthetic and natural apatites, Biomaterials 28 (2007) 3043–3054.

[36] Z. Chi, X.G. Chen, J.S.W. Holtz, S.A. Asher, Uv resonance raman-selective amide vibrational enhancement: quantitative methodology for determining protein secondary structure, Biochemistry 37 (1998) 2854–2864, https://doi.org/10.1021/bi971160z.

[37] L.C. Mayne, B. Hudson, Resonance Raman spectroscopy of N-methylacetamide: overtones and combinations of the C-N stretch (amide II′) and effect of solvation on the C=O stretch (amide I) intensity, J. Phys. Chem. 95 (1991) 2962–2967, https://doi.org/10.1021/j100161a006.

[38] W.E. Klee, G. Engel, IR spectra of the phosphate ions in various apatites, J. Inorg. Nucl. Chem. 32 (1970) 1837–1843.

[39] M.M. Figueiredo, J.A.F. Gamelas, A.G. Martins, Characterization of bone and bone-based graft materials using FTIR spectroscopy, in: infrared Spectrosc. Biomed. Sci., IntechOpen (2012).

[40] A.C. Chapman, D.A. Long, D.T.L. Jones, Spectra of phosphorous compounds—II.: the force constants of orthophosphates, Spectrochim. Acta. 21 (1965) 633–640.

[41] C. Rey, M. Shimizu, B. Collins, M.J. Glimcher, Resolution-enhanced fourier transform infrared spectroscopy study of the environment of phosphate ions in the early deposits of a solid phase of calcium-phosphate in bone and enamel, and their evolution with age. I: Investigations in thev 4 PO 4 domain, Calcif. Tissue Int. 46 (1990) 384–394.

[42] N.S. Chickerur, M.S. Tung, W.E. Brown, A mechanism for incorporation of carbonate into apatite, Calcif. Tissue Int. 32 (1980) 55–62.

[43] G. Piga, A. Santos-Cubedo, S.M. Solà, A. Brunetti, A. Malgosa, S. Enzo, An X-ray diffraction (XRD) and X-ray fluorescence (XRF) investigation in human and animal fossil bones from Holocene to Middle Triassic, J. Archaeol. Sci. 36 (2009) 1857–1868.

[44] M. Sponheimer, D. De Ruiter, J. Lee-Thorp, A.S. Späth, Sr/Ca and early hominin diets revisited: new data from modern and fossil tooth enamel, J. Hum. Evol. 48 (2005) 147–156, https://doi.org/10.1016/j.jhevol.2004.09.003.

[45] S. Kaciulis, G. Mattogno, L. Pandolfi, M. Cavalli, G. Gnappi, ˜ A Montenero, XPS study of apatite-based coatings prepared by sol-gel technique, n.d. www.elsevier.nlrlocaterapsusc (accessed February 28, 2020).

[46] E.O. López, A.L. Rossi, B.S. Archanjo, R.O. Ospina, A. Mello, A.M. Rossi, Crystalline nano-coatings of fluorine-substituted hydroxyapatite produced by magnetron sputtering with high plasma confinement, Surf. Coatings Technol. 264 (2015) 163–174, https://doi.org/10.1016/j.surfcoat.2014.12.055.

[47] E.O. López, A. Mello, H. Sendão, L.T. Costa, A.L. Rossi, R.O. Ospina, F.F. Borghi, J. G. Silva Filho, A.M. Rossi, Growth of crystalline hydroxyapatite thin films at room temperature by tuning the energy of the RF-magnetron sputtering plasma, ACS Appl. Mater. Interfaces 5 (2013) 9435–9445, https://doi.org/10.1021/am4020007.

[48] C. Viornery, Y. Chevolot, D. Léonard, B.O. Aronsson, P. Péchy, H.J. Mathieu, P. Descouts, M. Grätzel, Surface modification of titanium with phosphonic acid to improve bone bonding: characterization by XPS and ToF-SIMS, Langmuir. 18 (2002) 2582–2589, https://doi.org/10.1021/la010908i.

[49] W. Dreybrodt, Deposition of calcite from thin films of natural calcareous solutions and the growth of speleothems, Chem. Geol. 29 (1980) 89–105, https://doi.org/10.1016/0009-2541(80)90007-8.

[50] M. Oliveira, S. Hamilton, D. Calheiros, C. Jacobi, R. Latini, Modeling the potential distribution of the invasive golden mussel Limnoperna fortunei in the Upper Paraguay River system using limnological variables, Brazilian J. Biol. 70 (2010) 831–840, https://doi.org/10.1590/s1519-69842010000400014.

[51] L. Barbiero, S.A.C. Furquim, V. Vallès, S. Furian, A. Sakamoto, A.R. Filho, M. Fort, Natural Arsenic in Groundwater and Alkaline Lakes at the upper Paraguay basin, Pantanal, Brazil, n.d. https://hal.archives-ouvertes.fr/hal-00364414 (accessed February 20, 2020).

[52] S. Raynaud, E. Champion, D. Bernache-Assollant, P. Thomas, Calcium phosphate apatites with variable Ca/P atomic ratio I. Synthesis, characterisation and thermal stability of powders, Biomaterials 23 (2002) 1065–1072, https://doi.org/10.1016/S0142-9612(01)00218-6.

[53] M.J. Kohn, M.J. Schoeninger, W.W. Barker, Altered states: effects of diagenesis on fossil tooth chemistry, Geochim. Cosmochim. Acta 63 (1999) 2737–2747.

[54] P. Degryse, P. Muchez, B. De Cupere, W. Van Neer, M. Waelkens, Statistical treatment of trace element data from modern and ancient animal bone: evaluation of Roman and Byzantine environmental pollution, Anal. Lett. 37 (2004) 2819–2834.

[55] I.-M. Zougrou, M. Katsikini, F. Pinakidou, E.C. Paloura, L. Papadopoulou, E. Tsoukala, Study of fossil bones by synchrotron radiation micro-spectroscopic techniques and scanning electron microscopy, J. Synchrotron Radiat. 21 (2014) 149–160.

[56] P. Censi, P. Comin-Chiaramonti, G. Demarchi, A. Longinelli, D. Orue, Geochemistry and CO isotopes of the Chiriguelo carbonatite, Northeastern Paraguay, J. South Am. Earth Sci. 2 (1989) 295–303, https://doi.org/10.1016/0895-9811(89)90035-7.

[57] V.F. Velázquez, C. Riccomini, C. de B. Gomes, L. De Figuerado, C. Figueredo, Relacoes tectonicas do Magmatismo Alcalino do paraguai oriental, Rev. Do Inst. Geológico Sao Paulo. 19 (1998) 43–49.

[58] J.B. De Matos, Petrografía E Química Mineral De Ocorrencias Alcalinas De Provincia Alto Paraguay, UNIVERSIDADE DE SAO PAULO, Brasil-Paraguay, 2000.

[59] P. Comin-Chiaramonti, A. Marzoli, C. De Barros Gomes, A. Milan, C. Riccomini, V. F. Velázquez, M.M.S. Mantovani, P. Renne, C.C.G. Tassinari, P.M. Vasconcelos, The origin of post-Paleozoic magmatism in Eastern Paraguay, Spec. Pap. Geol. Soc. Am. 430 (2007) 603–633, https://doi.org/10.1130/2007.2430(29).

[60] C.B. Gomes, V.F. Velázquez, R.G. Azzone, G.S. Paula, Alkaline magmatism in the Amambay area, NE Paraguay: the cerro sarambí complex, J. South Am. Earth Sci. 32 (2011) 75–95, https://doi.org/10.1016/j.jsames.2011.04.004.

[61] P. Comin-Chiaramonti, A. De Min, V.A.V. Girardi, C.B. Gomes, Carbonatites and primary carbonates in the Rio Apa and Amambay regions, NE Paraguay, Lithos. 188 (2014) 84–96, https://doi.org/10.1016/j.lithos.2013.10.027.

[62] L. Merino, J. Morales, Mineralogía y geoquímica del esqueleto de los mastodontes de los yacimientos Batallones 1, 2 y 5. Implicaciones tafonómicas, Estud. Geol. 62 (2006) 53–64.